References

[1] X. Zhang and K. K. Mei, "Time-domain finite difference approach to the calculation of the frequency-dependent characteristics of microstrip discontinuities," *IEEE Trans. Microwave Theory Tech.*, vol. 36, pp. 1775–1787, 1988.

[2] J.-F. Lee, "Analysis of passive microwave devices by using three-dimensional tangential vector finite elements," *Int. J. Numerical Modelling: Elec. Netw., Dev. and Fields*, vol. 30, pp. 235–246, 1990.

[3] P. B. Johns, "A symmetrical condensed node for the TLM method," *IEEE Trans. Microwave Theory Tech.*, vol. MTT-35, pp. 370–377, 1987.

[4] R. H. Jansen, "The spectral-domain approach for microwave integrated circuits," *IEEE Trans. Microwave Theory Tech.*, vol. 33, pp. 1043–1056, 1985.

[5] R. W. Jackson, "Full wave, finite element analysis of irregular microstrip discontinuities," *IEEE Trans. Microwave Theory Tech.*, vol. 37, pp. 81–89, 1989.

[6] W. P. Harokopus and P. B. Katehi, "Characterization of microstrip discontinuities on multilayer dielectric substrates including radiation losses," *IEEE Trans. Microwave Theory Tech.*, vol. 37, pp. 2058–2065, 1989.

[7] S. B. Worm and R. Pregla, "Hybrid-mode analysis of arbitrarily shaped planar microwave structures by the method of lines," *IEEE Trans. Microwave Theory Tech.*, vol. MTT-32, pp. 191–196, 1984.

[8] R. H. Jansen and J. Sauer, "High-speed 3D em simulation for MIC/MMIC CAD using the spectral operator expansion (SOE) technique," *IEEE MTT-S Microwave Symp. Dig.*, Boston, 1991, pp. 1087–1090.

[9] A. Janhsen and V. Hansen, "Spectral analysis of multiport microstrip circuits with active and passive lumped elements," in *20th EUMC Rec.*, Budapest, Hungary, 1990, pp. 1053–1058.

[10] ——, "Modeling of planar circuits including the effect of space-varying surface impedances," *IEEE Microwave Guided Wave Lett.*, vol. 1, pp. 158–160, July 1991.

[11] J. M. Pond, C. M. Krowne, and W. L. Carter, "On the application of complex resistive boundary conditions to model transmission lines consisting of very thin superconductors," *IEEE Trans. Microwave*, vol. 37, 1989, pp. 181–190.

[12] R. K. Brayton and R. Spence, *Sensitivity and Optimization*. Amsterdam-Oxford-New York: Elsevier: 1980.

[13] T. E. Rozzi, J. H. C. van Heuven, and A. Meyer, "Linear networks as Möbius transformations and their invariance problems," *Proc. IEEE*, vol. 59, no. 5, pp. 802–803, 1971.

A High Frequency Model Based On The Physical Structure Of The Ceramic Multilayer Capacitor

L. C. N. de Vreede, M. de Kok, C. van Dam, and J. L. Tauritz

***Abstract*—In this paper modelling of the high frequency behavior of ceramic multilayer capacitors based on device physics is presented. An accurate predictive model incorporating physical dimensions, material constants and aspects of the CMC application environment is presented. This model is suitable for use in the design and development of improved high frequency CMC structures.**

I. Introduction

The physical modelling described in the following is primarily intended for the designer of high frequency ceramic multilayer capacitors (CMC's). Secondarily, users of CMC's can gain insight into the optimal placement of CMC's in their application environment.

Manuscript received September 27, 1991; revised March 10, 1992.

The authors are with the Delft University of Technology, Department of Electrical Engineering, Laboratory for Telecommunication and Remote Sensing Technology, P.O. Box 5031, 2600 GA Delft, The Netherlands.

IEEE Log Number 9200934.

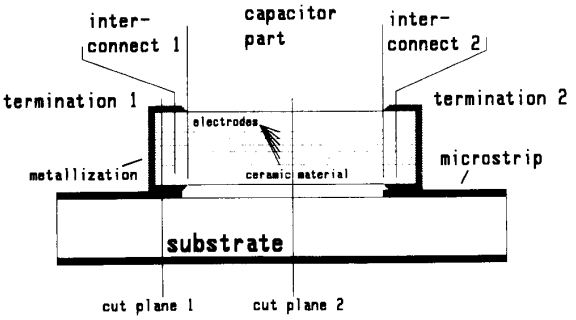

Fig. 1. Cross-section of CMC.

II. The Model

In 1991 Perna proposed a simple resonant folded transmission line model for a CMC mounted in series in a transmission line [1]. In 1987 Ingalls and Kent reexamined Perna's folded line model [2]. They tried to give the model a more rigorous basis and measured devices using the latest VNA's. This study has resulted in a more fundamental predictive model which has subsequently been proven in practice.

The structure under study is that of the intrinsic CMC mounted in an application environment as given in Fig. 1. It is clear from the figure that the capacitor conceptually consists of the following three regions:

The terminations:	connection of the electrodes and the metallization.
The interconnects:	interface between the terminations and the central capacitive region.
The capacitive part:	this is the actual capacitor consisting of a rectangular block of ceramic dielectric in which a number of interleaved precious-metal electrodes have been chosen to yield high capacitance per unit volume.

Transformation to an equivalent circuit model may be made by treating the electrodes and the terminations as multiconductor sections. This requires the accurate calculation of the multiconductor parameters. The device simulator PISCES has been used to carry out these computations [3]. In our case its use is limited to the calculation of the capacitance per unit length between the conductors. These conductors are entered into the program as cross-sections separated by ideal insulating materials whose dielectric constants correspond to those of the CMC under consideration. Solutions are found in a two dimensional plane which somewhat restricts the validity of the model for complicated structures at higher frequencies (i.e. a 100 pF capacitor with 6 plates is accurately modelled up to 10 GHz, a similar 330 pF capacitor model is accurate up to about 9 GHz). This restriction lies in the fact that there are a small number of three dimensional discontinuity regions which can not be accurately calculated in this way.

Keeping these restrictions in mind, we can transform the physical structure into a HF equivalent circuit as shown in Fig. 2. In the capacitive section each electrode is represented by a conductor ref-

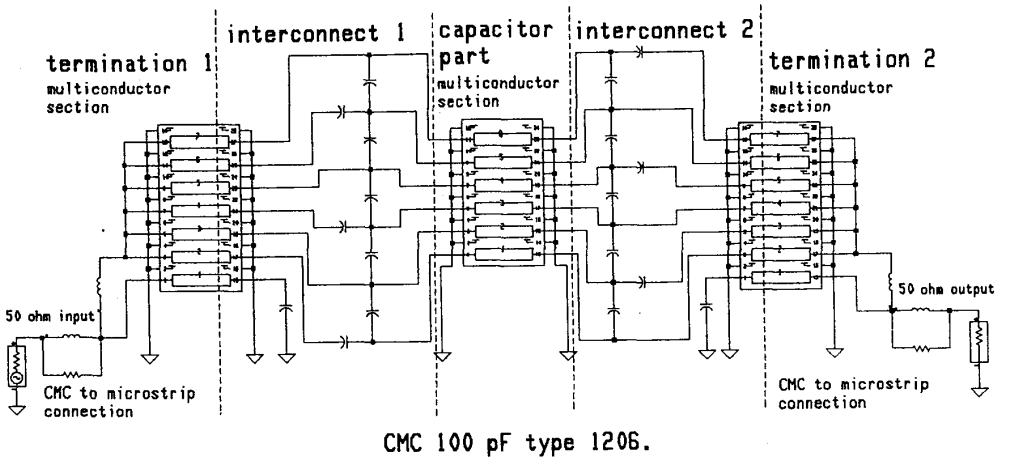

Fig. 2. Equivalent circuit of CMC.

erenced to the ground metallization of the substrate. The terminations are also modelled as multiconductor sections with one additional conductor symbolizing the termination metallization. A few extra elements describe the effects of the capacitor microstrip interface. The capacitors symbolize the stray capacitances at the end of the interrupted electrodes.

III. The Model Calculation

Once the constituent parts of the equivalent circuit have been determined frequency domain simulations can be carried out. We have appended the complete equivalent circuit model to an extended version of Hewlett Packard's Microwave Design System (MDS) installed in our laboratory. The Delft version of MDS enables the user to carry out parametric sweeps with self-defined circuit elements containing nearly an unlimited number of ports.

A. The Calculation of the Admittance Matrix with Losses

Formal solution of systems of coupled lossy transmission lines has been the subject of several publications [4]–[6]. Publications [5] and [6] include formulations suitable for straight forward computer implementation.

For the calculation of the admittance matrix the following assumptions have been made:

The mode of propagation is TEM for the homogeneous structure and quasi-TEM for the inhomogeneous structures. For both modes of propagation the field components (E and H) are transverse to the direction of propagation.

There are $(n + 1)$ coupled conductors one of which is the reference conductor.

All lines are uniform in the x-direction (Fig. 3).

All the required information is derived from the frequency-dependent line parameters (i.e. $\boldsymbol{R}$, $\boldsymbol{L}$, $\boldsymbol{G}$ and $\boldsymbol{C}$ matrices). The method takes into account frequency-dependent attenuation and dispersion.

B. The calculation of the matrices C, L, R *and* G

The $\boldsymbol{C}$ matrix for the multiconductor parts is determined using PISCES to solve the Poisson equation for the inhomogeneous cross sections. In order to reduce computing time only one half of the cross section has been used. PISCES calculates the capacitance matrix as well as equipotential lines. The equipotential lines may be of interest in the case of shielding problems as illustrated in Fig.

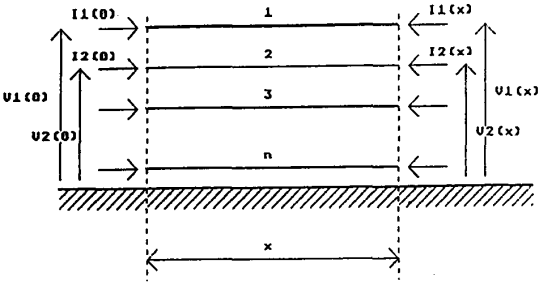

Fig. 3. N-coupled line system.

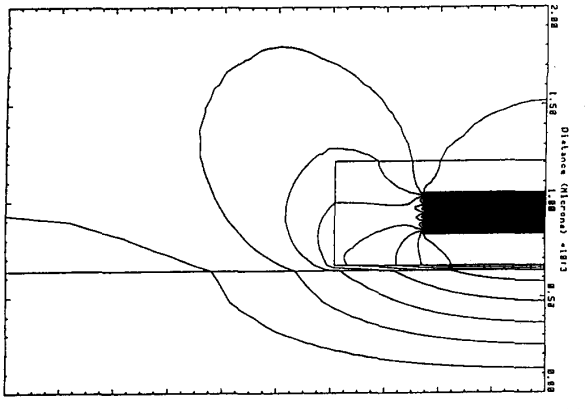

Fig. 4. Equi-potential lines calculated using PISCES for a capacitor with six electrodes (The electrodes are alternately connected to +10 and 0 V).

4. In this figure the equipotential lines have been plotted for the left side of cut plane 2 (figure 1) of the 100 pF CMC. The capacitor electrodes are alternately connected to +10 V and 0 V. The bottom of the substrate is grounded. The smoothness of the curves gives an indication of the mesh discretization. Note the concentration of field lines in the air layer under the capacitor. For the termination sections an additional solution is required for the cross section at cut plane 1 (Fig. 1).

Assuming small losses the $\boldsymbol{L}$ matrix can be determined from the $\boldsymbol{C}$ matrix for the homogeneous case.

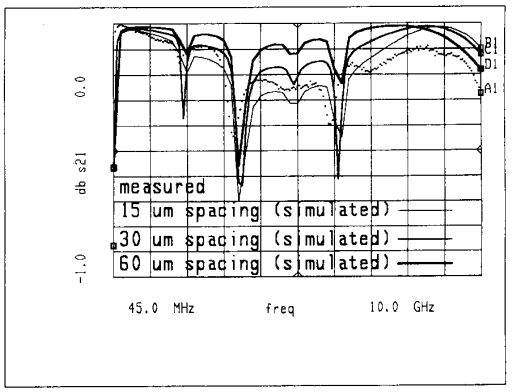

Fig. 5. Measured and simulated values of s21 for a 100 pF 1206 CMC capacitor with the distance of the capacitor to the substrate taken as parameter.

The $\boldsymbol{R}$ matrix must be computed from the $\boldsymbol{L}$ matrix using perturbational techniques for frequencies for which the skin effect dominates, in combination with low frequency solutions which take into account the presence of substantial internal inductance [7]. We have assumed that all conductors share the same cross section. This is correct for the electrode structure as given in Fig. 1 with the exception of the metallization caps of the terminations.

In our simulations $r(j\omega)$ has been taken equal to the dc resistance of the electrodes. Trial simulations with frequency dependent matrices have proved consistent with the results reported here.

The $\boldsymbol{G}$ matrix, which principally reflects dielectric loss, was set to zero for all elements, since the conductor loss dominates for the dielectrics in question.

IV. Simulation Results

In this section the use of CMC model will be illustrated.

In Fig. 4 the concentration of the equipotential lines in the air layer under the capacitor is noteworthy. This has been further explored in Fig. 5. In this figure the measured response is compared with simulated responses for spacings of 15, 30 and 60 μm between the capacitor and the substrate. It is evident that the thickness of the air layer influences the intensity of the resonances and the matching of the component in a 50 ohm environment.

Since the application environment influences the parameters of the multiconductor sections, orientation dependent effects should be simulated. The orientation dependent behaviour of odd resonances for the same type CMC mounted on its side as in Fig. 6 has been measured and calculated (Fig. 7). Note in Fig. 7 the remarkable change in field distribution. For the calculation of the frequency response the same circuit has been used as for the results in Fig. 5, with the exception of the $\boldsymbol{Y}_{2n}$ matrix of the multiconductor sections which has been modified to reflect the new orientation of the capacitor. The result is given in Fig. 8. Comparison of Figs. 5 and 8 illustrates a change in the number of resonances and their intensity. Measured results corroborate the calculations. The result found here is at variance with the conclusions drawn in [2]. In [2] the changes in the resonances are explained as the result of distributed excitation of the capacitor electrodes. In our model, however, the effects as described are clearly dependent on the multiconductor parameter matrices $\boldsymbol{C}$, $\boldsymbol{L}$, $\boldsymbol{G}$ and $\boldsymbol{R}$. In our method $\boldsymbol{G}$ and $\boldsymbol{R}$ do not change, which leads to the conclusion that the effect is dictated by the change in stray capacitances of the capacitor electrodes with respect to the application.

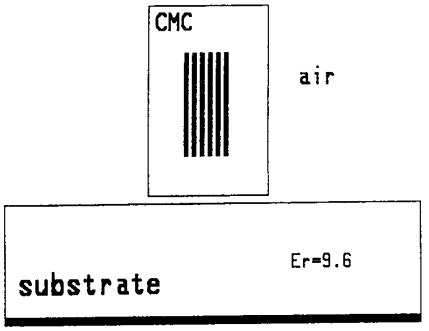

Fig. 6. Cross-section of a CMC mounted on its side over a substrate.

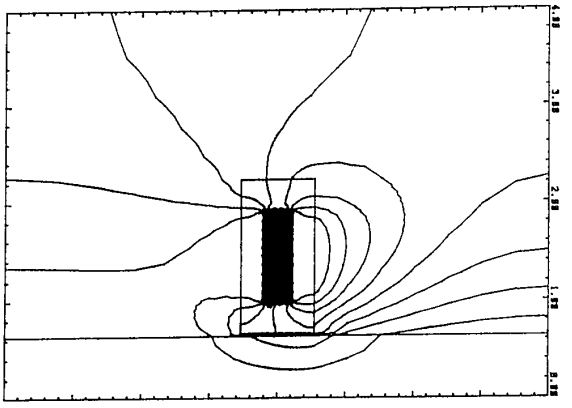

Fig. 7. Equi-potential lines for a side mounted CMC.

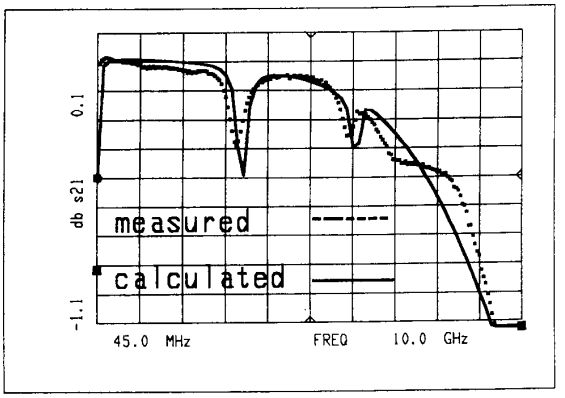

Fig. 8. Calculated and measured values of s21 for a capacitor as in Fig. 7 mounted on its side.

Conclusion

Significant progress has been made in the area of CMC modeling. It is now possible to accurately predict high-frequency behaviour of CMC structures based on physical modelling. Resonances are neither restricted to periodicity or monotonic amplitude decrease in frequency. At present the following factors can be taken into account:

electrode dimensions (length, width and thickness),
the inner structure of the CMC,

the measurement environment,
the dielectric constants,
the losses in the electrodes,
CMC microstrip effects.

Future effort will be devoted to incorporating frequency dependent loss mechanisms in the electrodes and dielectric layers. Companion publications dealing with computational aspects of the capacitor model, characterization and analytic modelling are in preparation.

ACKNOWLEDGMENT

The authors wish to acknowledge the support of Philips Components, Roermond. In particular Dr. H. A. Post, Dr. G. M. Stollman, Dr. P. E. C. Franken and ing. R. v. Ark have made this work possible.

REFERENCES

[1] V. F. Perna, Jr., "Chip capacitor dielectric effects on hybrid microwave amplifiers," in *ISHM Conf. Rec.*, Oct. 1971.
[2] M. Ingalls and G. Kent, "Monolithic capacitors as transmission lines," *IEEE Trans. Microwave Theory Tech.*, vol. MTT-35, pp. 964-970, Nov. 1987.
[3] *Manual TMA-PISCES-2B*, "Two-dimensional device analysis program," Version 8908, Technology Modelling Associates Inc., Feb. 15, 1989.
[4] L. A. Pipes, "Direct computation of transmission matrices of electrical transmission Lines, Part 1," *J. Franklin Inst.*, vol. 281, Apr. 1966.
[5] C. R. Paul, "On uniform multimode transmission lines," *IEEE Trans. Microwave Theory Tech.*, vol. MTT-21, pp. 556-558, Aug. 1973.
[6] A. J. Groudis and C. S. Chang, "Coupled lossy transmission line characterization and simulation," *IBM J. Res. Develop.*, vol. 25, pp. 25-41, Jan. 1982.
[7] T. R. Arabi, T. K. Sarkar, and A. R. Djordjevic, "Time and frequency domain characterization of multiconductor transmission lines," *Electromagnetics*, vol. 9, pp. 85-112, 1989.

Unified Dispersion Model for Multilayer Microstrip Line

A. K. Verma and G. Hassani Sadr

***Abstract*—A unified dispersion model is presented to calculate frequency dependent dielectric constant for a multilayer microstrip line. The model is a combination of TTL method, the method for the reduction of multilayer structures to an equivalent single layer microstrip line and the Kirschning and Jansen dispersion model. The result of the model has been confirmed within an accuracy of 1% against the results from SDA, ESDT and MM i.e., various forms of full wave analysis. These results have been confirmed between 2 GHz and 18 GHz. The present model is suitable for use in a CAD package for MIC, MMIC, and printed antenna design.**

I. INTRODUCTION

The microstrip transmission line is dispersive in nature. Many rigorous theoretical formulations have been reported in the literature to obtain $\epsilon_{eff}(f)$ of the microstrip line [1]-[3]. However, the published numerical results even on the same structure, show wide variations. The main cause of the variation in results is the tendency to reduce computer time by taking a small number of basis functions. Thus, an accurate full-wave field analysis is suitable for scientific investigation and generation of a data bank, but is not suitable for use in the CAD directly. Also, computation based on a full-wave analysis with the time saving mentioned above may not be accurate.

The closed form dispersion models for the microstrip line have been proposed by various researchers for MIC and MMIC CAD. Recently, the Kirschning and Jansen (KJ) dispersion model [4] has been found to be the most accurate compared against the measured values [5]. However, none of the researchers has reported on the dependence of the overall accuracy of the KJ dispersion model and other dispersion models on the calculation of $\epsilon_{eff}(0)$ by various static methods. Moreover, our careful analysis of experimental results of Edwards and Owens [6] using the KJ dispersion model shows a degradation of results for very narrow lines. In the first part of this paper we have compared various static methods to calculate $\epsilon_{eff}(f = 0)$ with the aim of improving the accuracy of the KJ dispersion model. In the second part of the paper, we have extended the KJ dispersion model to the multilayer microstrip line. The proposed "unified dispersion model" has been used to analyze $\epsilon_{eff}(f)$ for a double layer substrate on GaAs, shielded microstrip line and covered microstrip line. Results of the proposed model have shown good agreement with calculations carried out using SDA [1], ESDT [2] and the method of moments [3].

II. COMPARISON OF STATIC METHODS FOR DETERMINATION OF $\epsilon_{eff}(0)$

Kirschning and Jansen [4] have adopted the following mathematical structure for calculating the frequency dependent effective dielectric constant,

$$\epsilon_{eff}(f) = \epsilon_r - \frac{\epsilon_r - \epsilon_{eff}(f = 0)}{1 + P(f)}. \tag{1}$$

The accuracy of the dispersion expression (1) depends upon the accuracy of the determination of $\epsilon_{eff}(0)$. The static effective dielectric constant can be determined by methods developed by Bryant and Weiss [7], Hammerstad and Jensen [8], Wheeler [9] and Yamashita and Mitra [10]. Edwards and Owens [6] have carefully measured, between 2 GHz and 18 GHz the dispersion of microstrip lines on a sapphire substrate [$\epsilon_{r\perp} = 9.4$, $\epsilon_{r\parallel} = 11.6$, $h = 0.5 \pm 0.05$ mm] having w/h ratio between 0.1 and 9.14. For the purpose of comparison of $\epsilon_{eff}(0)$ calculated by four methods, the experimental values of ϵ_r and $\epsilon_{eff}(0)$ have been obtained from Edwards and Owens. The absolute value of percentage deviation of the calculated $\epsilon_{eff}(0)$ from the measured $\epsilon_{eff}(0)$ is defined as

$$K = \left| \frac{\epsilon_{eff}(0)\ \text{exp} - \epsilon_{eff}(0)\ \text{cal}}{\epsilon_{eff}(0)\ \text{exp}} \right| \times 100. \tag{2}$$

Fig. 2 shows a significant variation in the percentage deviation or percentage error for four methods. The rms deviation of $\epsilon_{eff}(0)$ obtained from the methods of Bryant and Weiss, Hammerstad and Jensen, Variational and Wheeler are 0.13%, 0.46%, 0.08% and 0.16% respectively. Thus, Bryant and Weiss and variational methods provide the best results. The method of Hammerstad and Jensen results in deviations as high as 3% for narrow lines. The variational method gives a higher deviation for a wider strip con-

Manuscript received October 10, 1991; revised January 30, 1992.
The authors are with the Department of Electronic Sciences, University of Delhi, India.
IEEE Log Number 9108324.